

# Topochemical and Electron Microscopic Analyses on the Lignification of Individual Cell Wall Layers During Wood Formation and Secondary Changes

Gerald Koch and Uwe Schmitt

**Abstract** The topochemical distribution of lignin and phenolic extractives in wood cell walls is determined on a cellular level by using scanning UV microspectrophotometry (UMSP) and transmission electron microscopy (TEM). These improved cellular analytical techniques enable direct imaging of the lignin distribution within individual cell wall layers during wood formation and secondary changes. The UMSP technique is based on the ultraviolet illumination of semithin transverse sections which can be related semiquantitatively to the concentration of lignin. Electron microscopy is variously used to obtain high-resolution information on the lignin distribution in wood cell walls which can be visualised by staining with potassium permanganate (KMnO<sub>4</sub>). By applying these improved techniques, (1) the topochemistry of lignification in developing xylem and wood tissue after wounding, (2) the topochemical detection of phenolic extractives, and (3) the lignin distribution in tropical bamboo species are presented and illustrated in detail. The described methods and presented results demonstrate that cellular UV microspectrophotometry and electron microscopy are ideally suited to study the topochemical distribution of lignin and phenolic extractives on a subcellular level. In particular, the application of the UV-scanning technique enables a direct imaging of lignin distribution (geometrical resolution of 0.25 µm × 0.25 µm) and provides fundamental information on the topochemistry of lignification. The techniques can be used for a wide range of applications in wood biology and wood topochemistry.

---

G. Koch (✉) • U. Schmitt

Thünen Institute of Wood Research, Leuschnerstr. 91, 21031 Hamburg, Germany  
e-mail: [gerald.koch@ti.bund.de](mailto:gerald.koch@ti.bund.de); [uwe.schmitt@ti.bund.de](mailto:uwe.schmitt@ti.bund.de)

# 1 Introduction

## 1.1 Lignin: Significance and Occurrence

Next to cellulose, lignin is the most abundant and important polymeric organic substance in plants. It is a characteristic chemical and morphological component of the tissue of higher plants such as pteridophytes and spermatophytes (gymnosperms and angiosperms), where it typically occurs in the vascular tissue, specialised for liquid transport and mechanical strength (e.g. Fengel and Wegener 1989). The lignin content in different plants is quite variable (Table 1). While in wood species the lignin content ranges from 20 to 40 %, aquatic and herbaceous angiosperms as well as many monocotyledons are less lignified (Sarkanen and Hergert 1971). Additionally, the distribution of lignin within the cell wall and the lignin content of different parts of a tree is not uniform. For example, high lignin amounts are characteristic for softwood branches and compression wood (Timell 1986), whereas the so-called gelatinous layers of tension wood fibres in hardwoods may be almost devoid of lignin (Timell 1969; Novaes et al. 2010).

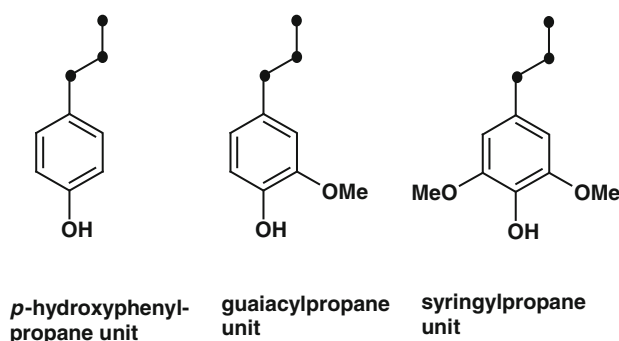
## 1.2 Chemical Structure of Lignin

The topochemical and electron microscopic study of cellular lignin distribution generally requires basic information on the chemical structure and composition of lignin.

Lignin is a complex phenolic polymer formed by radical coupling reactions of mainly three hydroxycinnamyl alcohols or monolignols (Fig. 1): *p*-coumaryl (4-hydroxycinnamyl), coniferyl (3-methoxy-4-hydroxycinnamyl) and sinapyl (3,5-dimethoxy-4-hydroxycinnamyl) alcohol, which are synthesised via the phenylpropanoid pathway (e.g. Nimz 1981; Boerjan et al. 2003). The complex structure of lignin arises from its biosynthesis in which the last step is a nonenzymatic, random recombination of phenoxy radicals of coniferyl, sinapyl and *p*-coumaryl alcohols. The synthesis of the monolignols (precursors) and the formation of lignin macromolecules comprise complicated biochemical and chemical reactions which have been extensively studied and repeatedly reviewed (e.g. Sarkanen and Hergert 1971; Glasser 1980; Terashima et al. 1993; Boerjan et al. 2003). According to Terashima (2000), the polymerisation of the monolignols is considered to proceed primarily via the following steps: (1) the formation of monolignol radicals by hydrogen peroxide and peroxidase or laccase and oxygen (Dean and Eriksson 1994), (2) the production of dilignols and dilignol quinone methides by coupling of the radicals, (3) the addition of water, lignol or carbohydrates to the quinone methides (Sarkanen and Hergert 1971; Higuchi 1997), (4) formation of phenyl radicals on oligo- and poly(lignols), and coupling with monolignol radicals to synthesise the poly(lignol). The mode of polymerisation

**Table 1** Chemical composition of different plants (adopted from Klemm et al. 2002)

Source	Composition (%)			
	Cellulose	Hemicelluloses	Lignin	Extract
Hardwood	43–47	25–35	16–24	2–8
Softwood	40–44	25–29	25–31	1–5
Bagasse	40	30	20	10
Coir	32–43	10–20	43–49	4
Cotton	95	2	1	0.4
Hemp	70	22	6	2
Jute	71	14	13	2
Sisal	73	14	11	2
Wheat straw	30	50	15	5

**Fig. 1** Molecular structure of the basic phenylpropane units of lignin

can be affected by relative amounts of radical types participating in the reaction. The first products of the coupling of monolignol radicals are  $\beta$ -O-4,  $\beta$ -5, and  $\beta$ - $\beta$  dimers (Fig. 2), whereas in the next stages of polymerisation, bulk type oligomers and endwise polymers are formed. As a result, a globular macromolecule is formed which is composed of bulk polymers inside and endwise polymers in the outer part (Terashima et al. 1998).

Variations in the chemical reactivity of lignin are based on the proportions of the three monolignol structural units (guaiacyl (G), syringyl (S), and *p*-hydroxyphenyl (H) units) in different wood species as well as in different tissues and even cell wall layers. Whereas softwood lignin consists mainly of guaiacylpropane (4-hydroxy-3-methoxyphenylpropane) units (G), hardwood lignins also contain up to 50 % syringyl (3,5-dimethoxy-4-hydroxyphenyl) groups (S). Guaiacyl lignins (G lignins) are predominantly polymerisates of coniferyl alcohol, while guaiacyl–syringyl–lignins (GS lignins) are composed of varying parts of the aromatic nuclei guaiacyl and syringyl in addition to small amounts of *p*-hydroxyphenyl units.

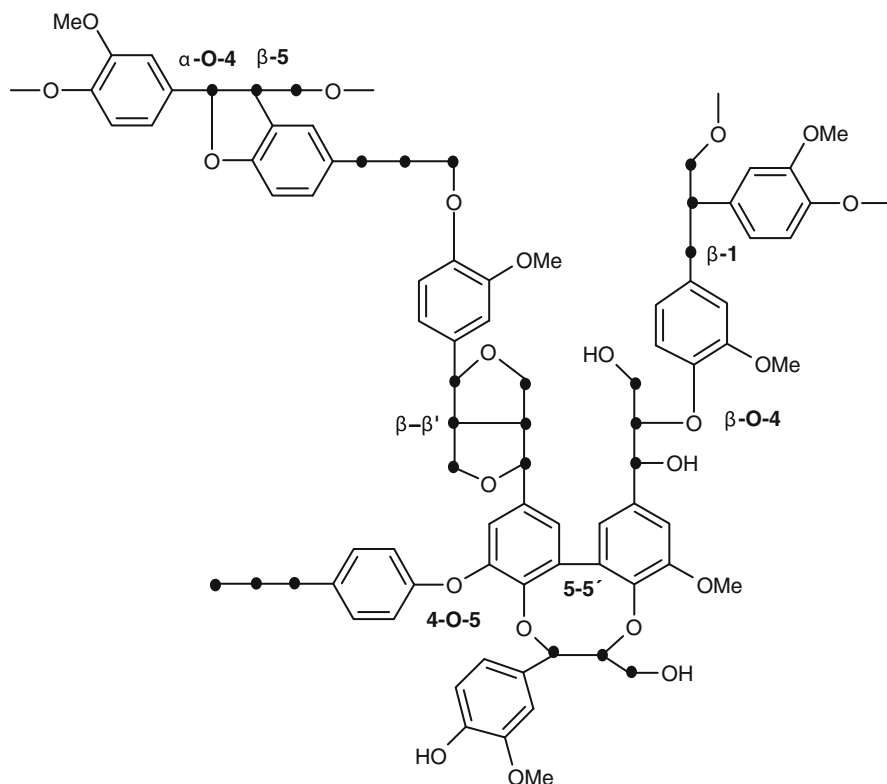
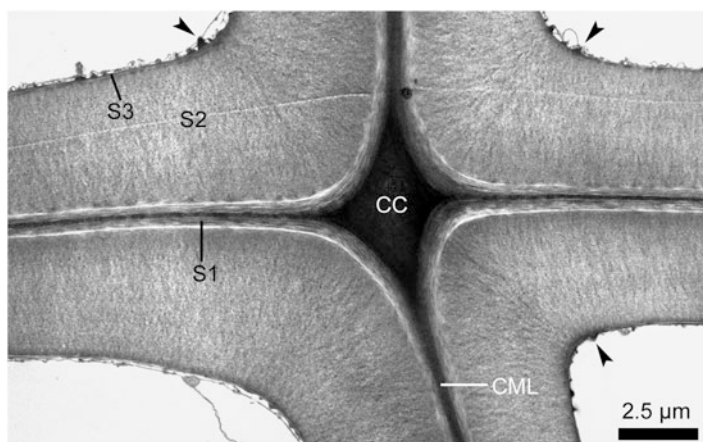


Fig. 2 Model of important lignin linkages (modified model adopted from Kindl 1991)

## 2 Deposition of Lignin Within the Polysaccharide Cell Wall Framework

### 2.1 Lignification of the Wood Cell Wall

Wood cell walls are strictly concentrically layered which is very well visible with the electron microscope especially in softwood tracheids. According to numerous wall models (review, see Brändström 2001), the individual wall layers are named in a common way (Fig. 3). The outermost wall portion connecting two neighbouring cells is called middle lamella (ML), followed by the primary wall (P) on both sides. ML and P form the so-called compound middle lamella (CML) because of their uniform appearance in the electron microscope. Well discernable from the CML is the secondary wall which is divided in the narrow and outermost S1 layer, the broad S2 layer, and the tiny, sometimes hardly visible innermost S3 layer. Some species (soft- and hardwoods, such as pine, fir and beech) additionally deposit a warty layer as the innermost wall portion. The middle lamella becomes distinctly broadened



**Fig. 3** TEM micrograph of fir (*Abies alba*) xylem after potassium permanganate staining. Cell corner region (CC) of four neighbouring tracheids. Typical cell wall layering with compound middle lamella (CML), secondary wall layers S1, S2 and S3 as well as a warty layer (arrowheads) deposited onto the S3

where more than two cells are in direct contact to each other; the name for this region is cell corner (CC). During wood formation, the incorporation of lignin within the polysaccharide cell wall framework is generally regarded as the final stage of the differentiating process of the typical secondary xylem cell wall. Results from ultraviolet, fluorescence and light autoradiographic microscopic studies as well as from electron microscopic studies have confirmed that lignin is most probably deposited initially in the cell corners when the surface enlargement of the cell is completed, and just before the S1 starts thickening. Lignification proceeds in the ML and the primary wall, starting at the tangential walls and spreading centripetally (Takabe et al. 1981). Lignification of the CML continues during the differentiation of the S1 and S2 layers, and even until the formation of the S3. Lignification of the secondary wall layers proceeds slowly in a first stage but becomes more rapid after formation of the S3 wall has been completed (Takabe et al. 1981). These findings indicate an ongoing lignification process throughout the entire period of cell wall differentiation, with a considerable delay as regards the synthesis of cellulose and hemicelluloses (Fig. 4).

On the ultrastructural level, Ruel et al. (1999) and Ruel (2004) added details using the immunogold-labelling technique to differentiate between condensed and non-condensed lignin subunits during deposition. The authors clearly demonstrated the micro-heterogeneity of lignification within developing wood cell walls. For fibres of hardwoods, they showed a preferable deposition of non-condensed GS lignins in the S1 and outer S2 layer and the incorporation of condensed GS subunits with a rather weak labelling in the S1 and within the entire S2 layer. According to Joseleau et al. (2004) as well as Lehringer et al. (2007, 2009) and in contrast to textbook knowledge, which is describing the G-layer consisting of only

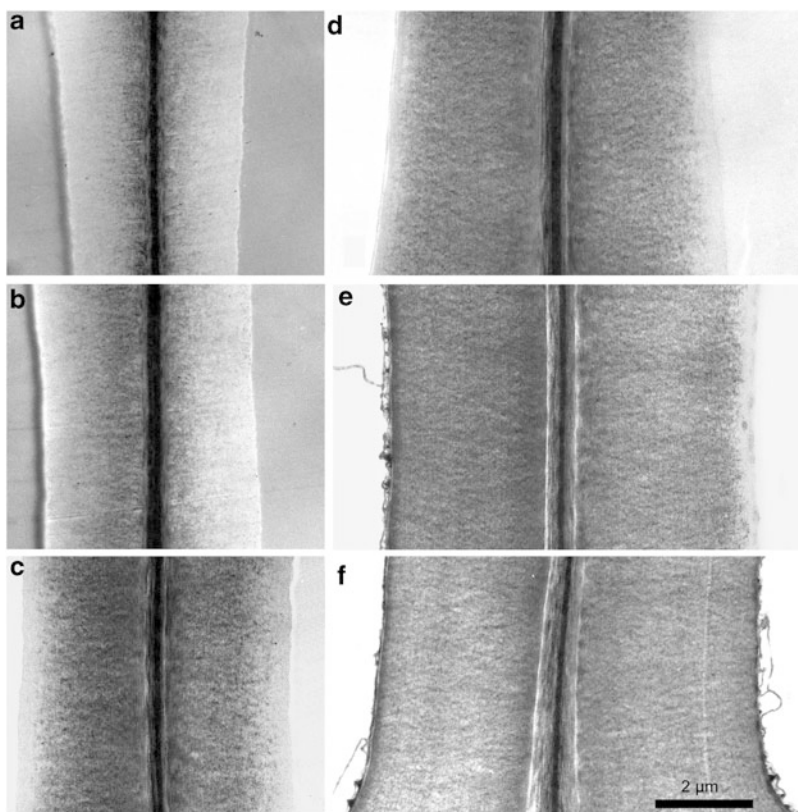


**Fig. 4** TEM micrographs of developing tracheid walls in fir (*Abies alba*), potassium permanganate staining. (a) Secondary wall still developing, lignification of middle lamella portions visible, outer secondary wall with early stage of lignification, inner secondary wall unlignified. (b) About one-third of the secondary wall lignified. (c) Advanced stage of the secondary wall lignification. (d) Lignification of the secondary wall nearly completed. (e) Lignification of the left wall appears completed, whereas the neighbouring right wall is still lignifying. (f) Completed lignification

polysaccharides, a low amount of lignin or lignin-like substances may be occasionally incorporated also in the gelatinous layer of tension wood fibres in hardwoods.

## 2.2 Deposition of Phenolic Extractives

In addition to its major structural components, i.e. cellulose, hemicelluloses and lignin, wood contains also an exceedingly large number of other low- and high-molecular organic compounds, the so-called accessory compounds or extractives. A major group of extractives (phenolic compounds) in hardwoods are the tannins and flavonoids ranging from simple phenols to condensed flavonoid systems which can

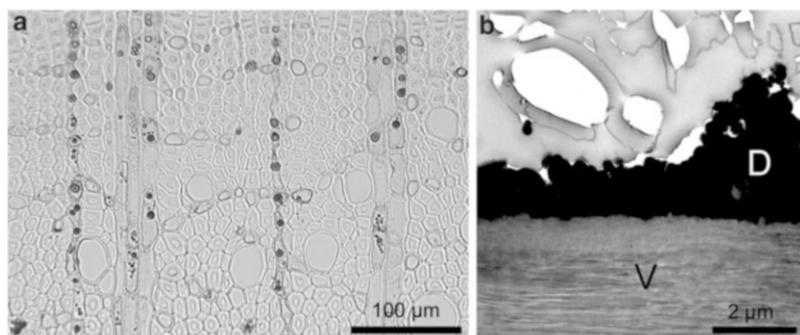


**Fig. 5** (a) Light micrograph of beech wood tissue (*Fagus sylvatica*) showing the deposition of high condensed phenolic extractives in the parenchyma cells (axial parenchyma and rays). (b) Deposition of crystalline extractives along the vessel wall of *Intsia bijuga* (V vessel wall, D deposits), TEM micrograph

also be topochemically analysed by UV-spectroscopy. The tannins are subdivided into hydrolysable tannins and non-hydrolysable or condensed tannins (phlobaphenes). The main components of the condensed tannins are the catechins (flavan-3-ols) and the leucoanthocyanidins (flavan-3,4-diols). They are often present in wood as colourless leuco-compounds and the colour will be secondarily developed by biochemical and chemical reactions (Koch 2003b). On the cellular level, the extractives are concentrated in the parenchyma cells (Fig. 5) and the resin canals; lower amounts are also found in the middle lamellae, intercellular spaces and cell walls of tracheids and libriform fibres (e.g. Grosser et al. 1974; Koch et al. 2003b) as well as occasionally also in vessel walls (Kleist and Schmitt 1999).

### 3 Topochemical Detection of Lignin by Using UMSP Technique and Electron Microscopy

#### 3.1 Application of UV Microspectrophotometry

Scanning UV microspectrophotometry (UMSP) has been established as a useful technique for the topochemical detection of lignin *in situ* and for its semiquantitative determination in the various layers of wood cell walls (Lange 1954; Fergus et al. 1969; Scott et al. 1969; Saka et al. 1982; Fukazawa 1992; Takabe 2002; Koch and Grünwald 2004). The technique is based on the ultraviolet illumination of semithin transverse sections of woody tissue. Lignin displays a characteristic ultraviolet absorbance spectrum with maxima around 212 nm and 280 nm due to the presence of associated phenylpropane groups with several chromophoric structural elements (Jaffé and Orchin 1962; Sarkanen and Hergert 1971; Hesse et al. 1991). No other component of the mature wood cell wall displays ultraviolet

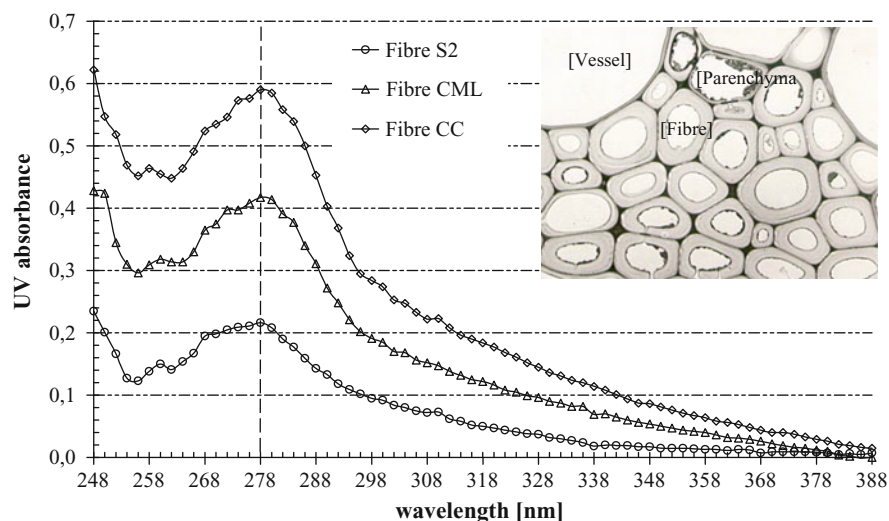


**Fig. 6** Representative UV absorbance spectra of individual cell wall layers in the woody tissue of *Fagus sylvatica* (fibre S2-secondary wall, CML-compound middle lamella, CC-cell corner)

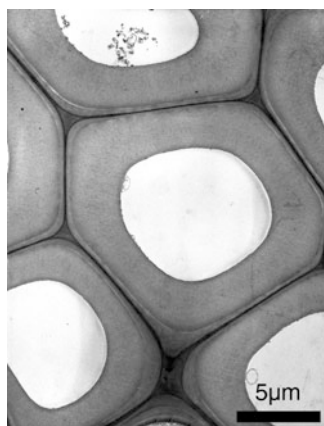
absorbance properties in the same spectral region, and the intensity of absorbance may therefore be related to the concentration of lignin across the cell wall. Furthermore, the UV absorbance maximum is sensitive to structural differences of the lignin allowing discrimination between hard- and softwood lignins due to different ratios of their guaiacyl- and syringylpropane units (Fergus and Goring 1970a, b; Takabe et al. 1992). Softwood lignin is mainly composed of guaiacylpropane units with an absorbance maximum at 280 nm, and the hardwood lignin consists of guaiacyl- and syringylpropane units in varying ratios characterised by a shifting maximum between 270 and 278 nm (Fig. 6) with lower wavelengths representing more syringyl units.

### 3.2 Application of Electron Microscopy

Electron microscopy was variously used to obtain high-resolution information on the lignin distribution in wood cell walls. Since the early 1980s, advanced electron microscopic techniques were developed to improve our knowledge on the lignin topochemistry. The bromination technique revealed lignin distribution by combination of electron dispersive X-ray analysis (EDXA) with transmission (TEM) or scanning electron microscopy (SEM) (e.g. Saka and Thomas 1982; Westermarck 1985; Donaldson and Ryan 1987). Either sectioned material or isolated wall fractions were analysed. This technique confirmed on a high-resolution level that middle lamella portions contain distinctly more lignin than secondary walls, whereby ratios between middle lamella and secondary wall lignin were determined.



**Fig. 7** TEM micrograph of oak (*Quercus* sp.) xylem showing several fibres with distinct wall layering after potassium permanganate staining (from Čufar et al. 2008)



Similar results were obtained with the mercurisation technique and subsequent SEM/TEM–EDXA analyses which is also based on chemical reactions between lignin and inorganic compounds (Eriksson et al. 1988; Westermark et al. 1988). For example, lignin contents for middle lamella portions of spruce wood were measured obtaining percentage values of 50–60 %.

According to the methods mainly developed by Hepler and Newcomb (1963), Parham (1974), Paszner and Behera (1989), as well as Michalowicz and Robert (1990), potassium permanganate became a very useful general staining agent for cell walls of soft- and hardwoods (Figs. 3, 4 and 7). Later on potassium permanganate was regularly applied especially for lignin localisation in walls of mostly softwood species (e.g. Maurer and Fengel 1991; Donaldson 1992; Singh and Donaldson 1999). However, potassium permanganate does not differentiate between guaiacyl- and syringylpropane units. Since a few years also field-emission scanning electron microscopy (FESEM) was sometimes used to reveal fine structural aspects of the cell wall architecture (Daniel et al. 2004; Lehringer et al. 2009). Fromm et al. (2003) succeeded in obtaining high-resolution micrographs of mercurised softwood tracheids; lignin complexes could be shown within the polysaccharide network using the backscattering mode of a FESEM.

### 3.3 Application of Immunogold Labelling

Another technique for ultrastructural lignin localisation in wood cell walls is the immunogold labelling with lignin-specific markers. Ruel et al. (1994) raised polyclonal antibodies against synthetic dehydrogenative polymers (DHPs) in rabbits for immunological lignin localisation. Visualisation of antibody binding sites by electron microscopy was achieved with a secondary marker coupled onto small gold particles (usually a protein A-gold complex) binding to the first marker. Those treatments resulted in good labellings of lignin in various cell wall types. Beside a

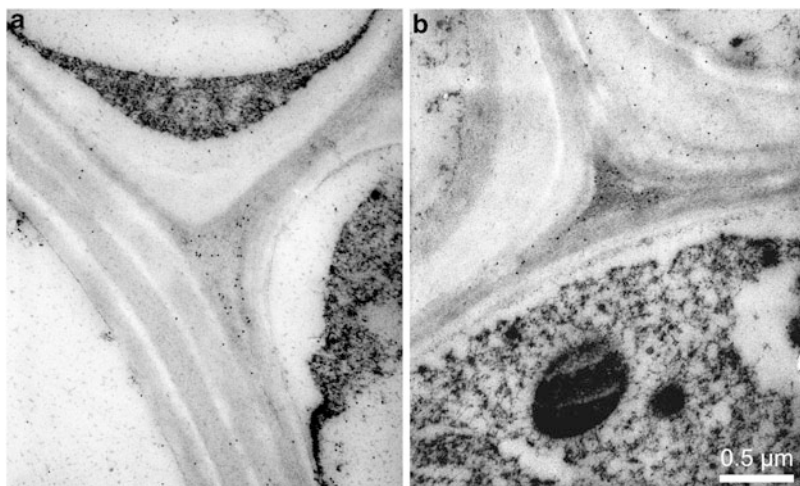


**Fig. 8** TEM micrographs of cell walls in developing xylem of poplar after immunogold labelling with antibodies against peroxidases. Early stages of fibre wall development (**a**) show a strong labelling with gold particles in cell corner regions, whereas later stages are characterised by a weak and more uniform labelling across the entire secondary wall (**b**)

direct lignin labelling, enzymes, such as peroxidases, laccases, or cinnamic acid-4-hydroxylases as key enzymes involved in the lignification of plant cell walls, were localised in developing walls with specific antibodies (Smith et al. 1994; Kim et al. 2002). Kim et al. (2002) localised peroxidases in developing xylem cells of *Populus*. Strong labelling of cell corner regions during early developing stages is probably confirming the onset of lignification in these wall portions (Fig. 8a). On the other hand, advanced stages of cell wall formation are characterised by a weak but more uniform labelling across the entire developing secondary wall (Fig. 8b) which is interpreted as evidence for an incorporation of peroxidases into a young secondary wall simultaneously with the deposition of the polysaccharide matrix.

Recently raised antibodies enabled a discrimination between non-condensed (O-4 aryl-alkyl bonds) and condensed (mainly C-C bonds) lignin interunit linkages (Joseleau and Ruel 1997). Kukkola et al. (2003, 2008) raised a polyclonal antibody against a specific condensed lignin substructure, i.e. the 8-ring dibenzodioxocin, for analysing details on the lignin composition in cell walls of softwood xylem. In addition to electron microscopy, Kukkola et al. (2004) applied confocal laser-scanning fluorescence microscopy and visualised dibenzodioxocin with antibodies coupled to a fluorescent dye. They found out that in mature xylem cells of birch and spruce, dibenzodioxocin was preferably located in the S3 layer of fibres and tracheids as well as in the entire secondary wall of birch vessels. Developing cells did not show any labelling. These results support the assumption that more condensed lignin subunits contribute to a higher stability particularly in vessel walls.

## 4 Experimental Approach of UV Microspectrophotometry and Electron Microscopy

### 4.1 Sampling and Preparation

The preparation and sectioning followed procedures normally employed for electron microscopy. First, small blocks (measuring about  $1 \times 1 \times 5 \text{ mm}^3$ ) of selected species are dehydrated in a graded series of acetone, impregnated with Spurr's epoxy resin (Spurr 1969) through a series of acetone/resin mixtures, followed by immersion in pure resin and polymerisation at  $70^\circ \text{C}$  for 24 h. For the investigation of low molecular phenolic extractives, a direct impregnation with pure Spurr's resin under vacuum was additionally developed. For this special impregnation, the specimens are freeze-dried and immediately embedded with Spurr's epoxy resin under mild vacuum with several cycles of evacuation and ventilation as described by Kleist and Schmitt (1999). The embedded blocks are trimmed to provide a face of approximately  $0.5 \text{ mm}^2$ . Semithin sections ( $1 \mu\text{m}$ ) are cut with an ultramicrotome using a diamond knife. The sections are then transferred to quartz microscope slides, immersed in a drop of non-UV absorbing glycerine and covered with a quartz cover slip. The UV microscopic investigations are carried out using the immersion ultrafluar objectives 32:1 and 100:1. All lenses are completely achromatic in the range of 200...700 nm. The immersion oil used consisted of a glycerine/water mixture  $n_D = 1.46$ .

### 4.2 Measuring Technique of Scanning UV Microspectrophotometry

The topochemical analyses are carried out using a UV microspectrophotometer (UMSP 80, Zeiss) equipped with a scanning stage enabling the determination of image profiles at defined wavelengths using the scan program APAMOS<sup>®</sup> (Automatic-Photometric-Analysis of Microscopic Objects by Scanning (Zeiss)). For the detection of the lignin distribution of softwoods and hardwoods, wavelengths of 280 nm and 278 nm, respectively, are selected. The scan programme digitises rectangular fields with a local geometrical resolution of  $0.25 \mu\text{m} \times 0.25 \mu\text{m}$  and a photometrical resolution of 4,096 grey scale levels which are converted in 14 basic colours to visualise the absorbance intensities. The scans can be depicted as two- or three-dimensional image profiles including a statistical evaluation (histogram) of the semiquantitative lignin distribution (Fig. 9).

The sections are also conventionally subjected to point measurements with a spot size of  $1 \mu\text{m}^2$  with varying wavelengths between 240 and 400 nm (comp. Fig. 6) using the program LAMBDA SCAN<sup>®</sup> (Zeiss). This program evaluates the UV absorbance spectra of the lignified cell walls and accessory compounds in tissues.

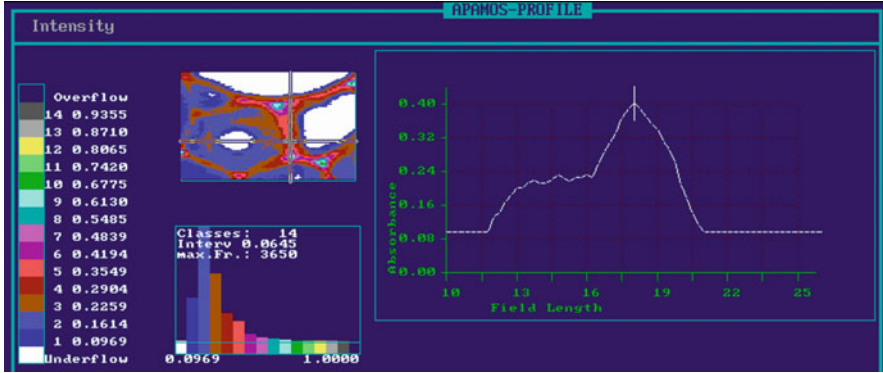


**Fig. 9** UV microscopic scanning profile of lignin distribution in beech wood tissue (cross section of individual cell wall layers). The colour pixels display the UV absorbance at 278 nm wavelength with a resolution of  $0.25 \mu\text{m} \times 0.25 \mu\text{m}$  (Röder et al. 2004)

The lignin concentrations are estimated according to the Lambert–Beer’s law:

$$\text{UV absorbance} = \varepsilon \cdot C \cdot d,$$

where  $\varepsilon$  is the extinction coefficient,  $C$  the volume concentration and  $d$  the thickness of the absorbing layer. Considering the cell wall in a cross section of  $1 \mu\text{m}$  thickness, the incident UV light intensity  $I_0$  is reduced to the intensity  $I_{\text{cell wall}}$  emerging from the cell wall due to the absorbance by the constituent lignin. Measurement of  $I_0$  is facilitated by the unchanged passage of the incident radiation through the embedding medium in the cell lumen.  $I_0$  may therefore be replaced by  $I_{\text{lumen}}$ , the intensity of UV light emerging from the lumen:

$$\text{UV absorbance} = \log I_{\text{lumen}}/I_{\text{cell wall}}.$$

### 4.3 Principle of Preparation for Transmission Electron Microscopy

For transmission electron microscopy (TEM) of woody material, in most cases, a low viscosity embedding resin is used. Spurr (1969) introduced such an epoxy resin with nonenyl succinic anhydride as the main component. Due to its excellent penetration also into woody tissue, it is still in use in many laboratories, although some components may nowadays be replaced by less harmful chemicals. Prior to embedding, the standard preparation of living plant tissue for TEM is an initial fixation with aldehydes followed by a second fixation with osmium tetroxide, which simultaneously acts as a staining agent for mainly membranes and cell walls.

**Fig. 10** TEM micrograph of mature xylem of birch (*Betula pendula* Roth) embedded in Spurr's epoxy resin and en bloc stained with osmium tetroxide. The entire tissue is well prepared and with an excellent contrast after uranyl acetate and lead citrate staining (F fibre, R ray, V vessel)

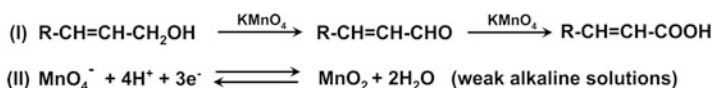
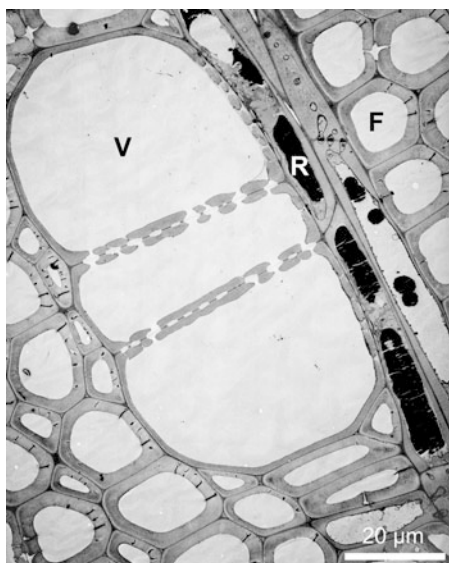


**Fig. 11** Diagram of the major pathway for  $\text{KMnO}_4$  stainings.  $\text{KMnO}_4$  probably oxidises the functional groups of the side chains of the lignin from the alcohol to the carboxylic acid (I).  $\text{MnO}_2$  is finally deposited on the sections (II) (modified from Schmitt and Melcher 2004)

Subsequent poststaining with uranyl acetate and lead citrate leads to an excellent visualisation of cytoplasmic constituents and cell walls (Fig. 10).

However, analyses of wood cell walls are often performed with material which is directly embedded in Spurr's epoxy resin without the application of fixatives (e.g. Schmitt et al. 2006, Čufar et al. 2008). There is often no need to preserve living cells. Sections produced from such material are routinely stained with potassium permanganate ( $\text{KMnO}_4$ ) which preferably reacts with lignin molecules and therefore indicates the lignin distribution in cross cell walls (see also Sect. 3.2). Schmitt and Melcher (2004) provided the chemical background of the staining process, which is based on the permanganate ion ( $\text{MnO}_4^-$ ) acting as a strong oxidant in acidic and alkaline solutions and in high dilutions.  $\text{KMnO}_4$  probably oxidises the functional groups of the alcohol of the lignin molecules to the aldehyde and carboxylic acid (Fig. 11). Finally, the resulting water-insoluble reaction product manganese dioxide ( $\text{MnO}_2$ ) is deposited on the ultrathin section visualising the reaction sites.

## 5 Application and Examples of Topochemical Detection of Lignin and Phenolic Extractives

### 5.1 *UV-Scanning Profiles of Lignin Distribution in Wood Cell Walls*

Scanning UV microspectrophotometry enables direct imaging of the lignin distribution within individual cell wall layers and incorporates advances on the previous UV microscopy investigations of lignin topochemistry. Figure 12 shows typical two- and three-dimensional UV image profiles of lignin distribution. The localisation of phenolic extractives in parenchyma cells is also shown (Fig. 13). The grey and colour scales indicate different intensities of UV absorbance at  $\lambda_{280\text{ nm}}$  and  $\lambda_{278\text{ nm}}$ . The high resolution ( $0.25\text{ }\mu\text{m} \times 0.25\text{ }\mu\text{m}$  per pixel) enables a high differentiation of the UV absorbance within individual cell wall layers.

The image profiles of spruce tracheids (Fig. 12a) are characterised by a high UV absorbance at the cell corners and compound middle lamellae ( $\text{abs}_{280\text{ nm}}$  0.61–0.87) as compared to the adjacent S2 layers with a lower, slightly varying lignin distribution ( $\text{abs}_{280\text{ nm}}$  0.35–0.54). As found by Lange (1954) and Fergus et al. (1969), the average lignin content in the compound middle lamella is about twice of that in the S2 of the tracheids. For detailed illustration, the scanning area is presented as a three-dimensional image as well as line image profile. In the three-dimensional profile, the compound middle lamella region stands out as a highly absorbing band which broadens towards a heavily lignified area at the cell corners. An example of a line image profile depicted by the marked cross line is shown in detail. The compound middle lamella of the scanned spruce tracheid is recorded as a pronounced peak while the S2 layers are characterised by a lower level on either side of the compound middle lamella. These graphical presentations allow a refined evaluation of the topochemical distribution of lignin within the cell walls. An unambiguous statistical presentation of the data is an additional asset.

The scanned beech fibre (Fig. 12b) shows a different absorbance level as compared to the softwood tracheids. In particular, the broad S2 layer displays a lower absorbance with values of  $\text{abs}_{278\text{ nm}}$  0.16–0.29. The uniform level of absorbance in this wall layer corresponds to earlier results reported by Saka and Goring (1988), who predicted that lignin distribution across the width of the whole S<sub>2</sub> should be homogeneous. The compound middle lamella is distinguished by higher absorbance values as compared to those of the spruce tracheid.

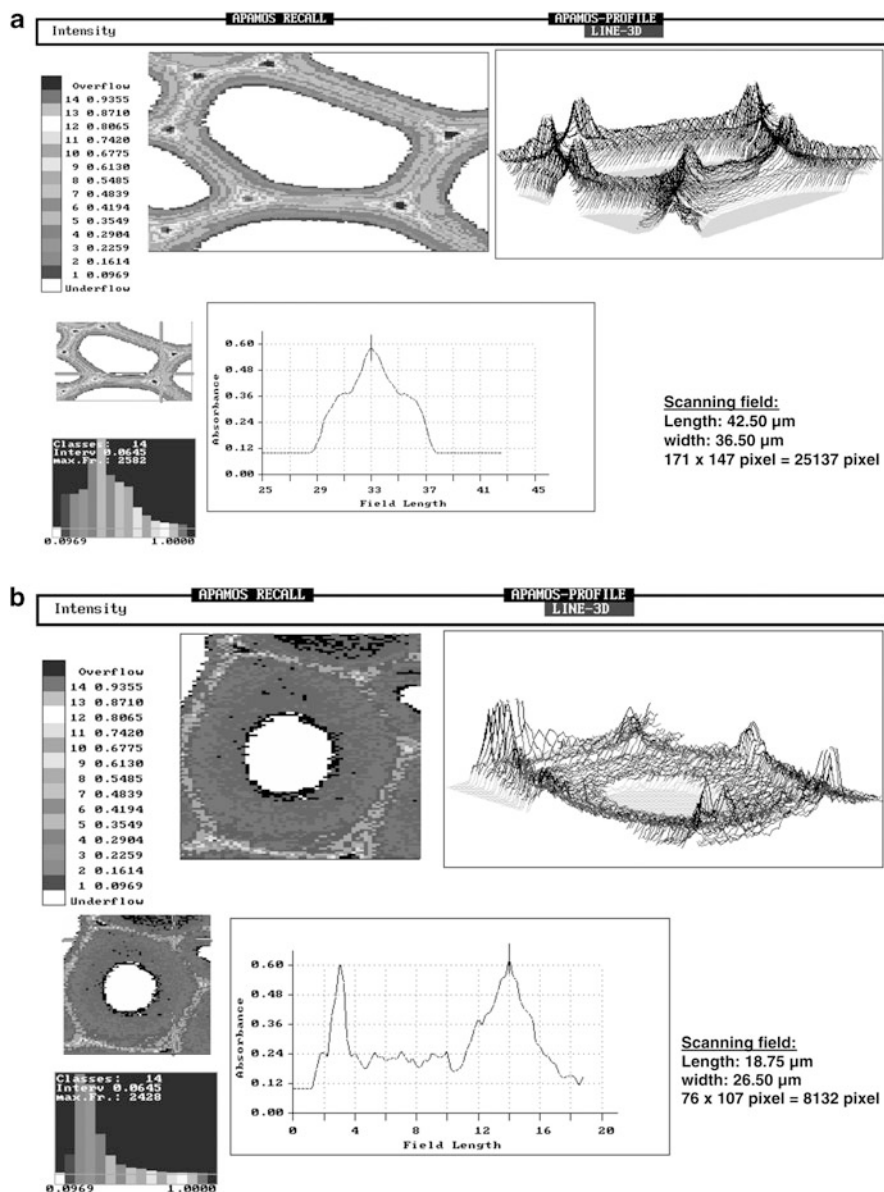


**Fig. 12** UV microscopic image profiles of an individual (a) tracheid of *Picea abies* and (b) fibre of *Fagus sylvatica* scanned with a geometrical resolution of 0.25  $\mu\text{m} \times 0.25 \mu\text{m}$ . The scales indicate the different UV absorbance values at a wavelength of 280 nm (absorbance maximum of softwood lignin) and 278 nm (absorbance maximum of hardwood lignin) (Koch and Grünwald 2004)



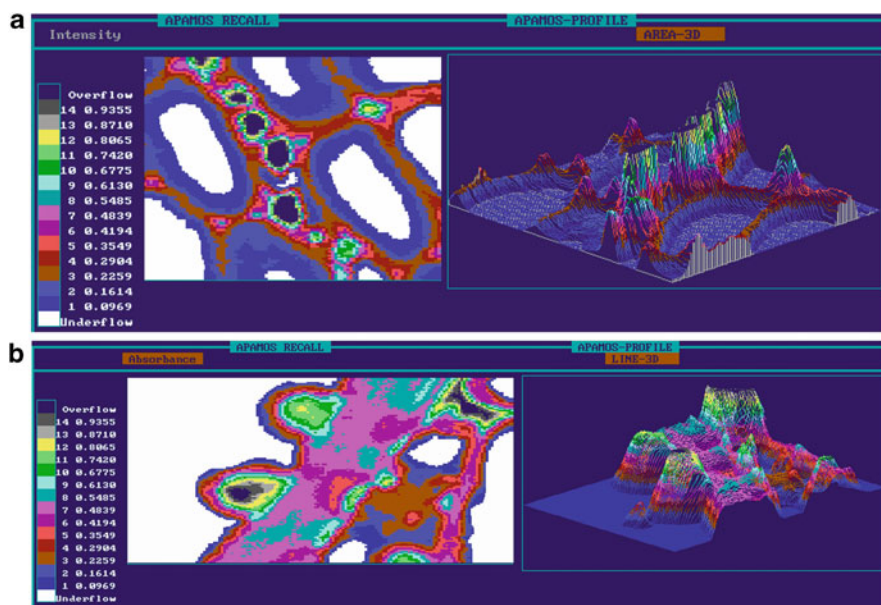


**Fig. 13** (a) UV microscopic image profiles of *Fagus sylvatica* tissue measured at  $\lambda_{278\text{nm}}$  showing the deposition of phenolic extractives (arrows) in lumina of ray parenchyma cells (Koch et al. 2003), (b) detailed UV microscopic scanning profiles of deposited crystalline extractives on the vessel wall and within the pit membranes of *Intsia bijuga*. The colour pixels represent different UV absorbance values measured at  $\lambda_{278\text{nm}}$  (Koch et al. 2006)

## 5.2 Topochemical Detection of Phenolic Extractives

Scanning UV microspectrophotometry can also be used to detect and quantify aromatic compounds associated with the woody tissue (Koch et al. 2003b). The presence of extractives can easily be visualised as spherical conglomerations of high absorbance as compared with the surrounding tissue. In Fig. 13a, the local deposition of extractives in the lumina of ray parenchyma cells of beech heartwood is emphasised by a significantly higher absorbance ( $\text{abs}_{280\text{nm}}$  0.68–1.00) as compared to the cell wall-associated lignins. The phenolic compounds are generally synthesised by parenchyma cells *in situ* and are highly condensed, making it impossible for them to penetrate into the interfibrillar spaces of the cell walls (Hillis 1987). The adjacent fibres do not seem to be impregnated, as evidenced by lower absorbance levels in these cells. The scanned fibres and parenchyma cells show the typical absorbance profile originating from the lignification of the different cell wall layers. In contrast to wood species with an obligatory heartwood formation, the cell walls of beech fibres are not impregnated, and the deposited phenolic extractives in the cell lumina do not contribute to an enhanced decay resistance (compare Koch and Kleist 2001; Kleist and Bauch 2001).



In addition, the topochemical distribution of phenolic deposits in the vessels of *afzelia* (*Afzelia* spp.) and *merbau* (*Intsia* spp.) heartwood was investigated by means of cellular UV microspectrophotometry (UMSP) in order to characterise the chemical composition and synthesis by pit membrane-associated enzymes (Koch et al. 2006). Figure 13b shows a detailed UV image profile of phenolic deposits, the vessel cell wall, and an associated parenchyma cell in *merbau* (*Intsia* spp.). The phenolic deposits as spherical conglomerations of high absorbance are silhouetted clearly against the surrounding vessel wall. Also here, the deposits are characterised by very high absorbances (0.7–1.0 overflow). Furthermore, on the outer part of the vessel S2, directly associated with the CML adjacent to an axial parenchyma cell, local high absorbance spots are detectable. These areas are localised in the pit canals and pit membranes. The UV intensities at 278 nm (0.7–0.9) of the pits are strong evidences for an impregnation of the membranes and pit canals with phenolic extractives.

### 5.3 UV-Absorbance Spectra of Lignin and Phenolic Extractives

The lignification of individual cell wall layers and the deposition of phenolic extractives can also be studied by the evaluation of UV absorbance spectra in a wavelength range of 240–400 nm. In Fig. 14, typical UV absorbance spectra of individual cell wall layers in beech are presented. The UV spectra of the compound middle lamellae and S2 show the typical absorbance behaviour of a hardwood lignin with a distinct maximum at 278 nm and a local minimum at about 250 nm (Fergus and Goring 1970a; Takabe et al. 1992). The cell wall layers of vessels are generally characterised by higher absorbance values than that of fibres. This behaviour is based on the different chemical composition of lignin in both cell types. Fergus and Goring (1970a, b) and Terashima et al. (1986) proved that the lignin located in vessel walls consists predominantly of the strongly absorbing guaiacyl type units, while the fibre wall lignin contains more syringyl units showing a lower UV absorbance with increasing  $\text{OCH}_3/\text{C}_9$  ratio (Musha and Goring 1975). In comparison, the UV spectra of spruce tracheids show generally higher absorbance values as compared to the hardwood fibres and vessels. A pronounced absorbance maximum at 280 nm usually indicates the presence of the strongly absorbing guaiacyl lignin (Musha and Goring 1975; Fujii et al. 1987).

The detected phenolic extractives in the ray parenchyma cells of beech heartwood have much higher absorbance values ( $\text{abs}_{280\text{nm}}$  0.75 and 0.95) than cell wall-associated lignins ( $\text{abs}_{280\text{nm}}$  0.20 and 0.38). Furthermore, their absorbance maxima display a bathochromic shift to a wavelength of 284 nm and a slight shoulder at a wavelength range of 320 nm. This spectral behaviour can be explained by the presence of chromophoric groups, e.g. conjugated double bonds. The higher degree of conjugation stabilises  $\pi-\pi^*$  transitions resulting in absorbance bands shifted to higher wavelengths (Goldschmid 1971) which can be detected by UV

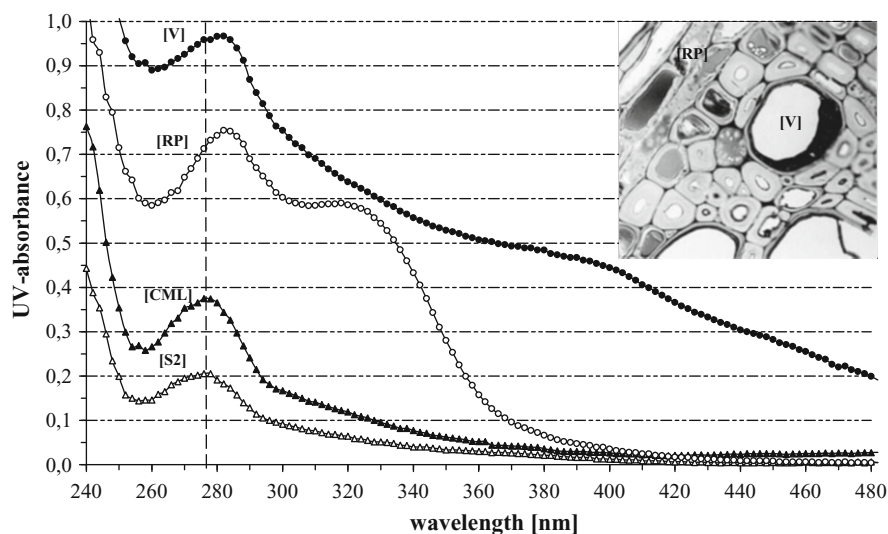


**Fig. 14** Representative UV absorbance spectra deposited phenolic compounds in the woody tissue of beechwood with red head (*open triangle*, low molecular phenolic compound in the secondary wall [S2], *open circle*, high condensed phenolic compound in the lumen of a ray parenchyma cell [RP], *filled circle*, high condensed phenolic compound in the lumen of a vessel [V], *filled triangle*, compound middle lamella of a fibre [CML]). UV photograph at 280 nm of discoloured beechwood tissue (Koch et al. 2003b)

microspectrophotometry. However, the technique does not allow the chemical identification of the condensed phenolic extractives (Koch et al. 2003a).

In the tropical wood species afzelia and merbau, the spectra of the phenolic deposits are characterised by a distinct absorbance maximum at 368 nm (Fig. 15). According to Hillis and Yazaki (1973), who have analysed the methanol–water extracts of the deposits in the cell lumen of merbau by high-performance liquid chromatography (HPLC), the deposits are composed of pure robinetin ( $C_{15}H_{10}O_7$ ) and kaempferol ( $C_{15}H_{10}O_2$ ). The UV spectrum of these both compounds has a distinct minimum at 280 nm. In this range, however, the lignified cell wall layers of vessels (Fig. 15 [3]) and fibres (Fig. 15 [4]) reveal a pronounced maximum due to the UV characteristics of the guaiacyl and syringyl units in lignin. Accordingly, lignin spectra can be basically distinguished from those of robinetin. The pit membranes and pit canals of associated vessel and parenchyma cells are impregnated by these compounds. These results verify the assumption that the synthesis of deposits in afzelia and merbau is regulated by means of pit membrane-associated enzymes.

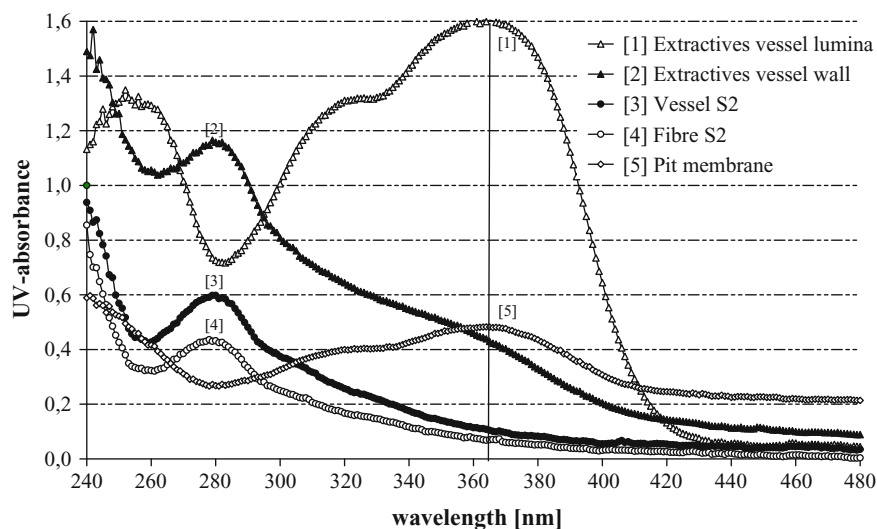


**Fig. 15** Representative UV absorbance spectra of individual cell wall layers (S2 of a vessel and a fibre), phenolic extractives deposited in vessel lumen, and extractives impregnating the vessel wall and pit membranes of *Intsia bijuga* (Koch et al. 2006)

#### 5.4 Topochemical Investigations on Cell Walls in Developing Xylem of Beech

Cell wall thickening and lignification of beech xylem (*Fagus sylvatica* L.) were determined by means of light microscopy, cellular UV microspectrophotometry and transmission electron microscopy. It could be clearly demonstrated that the differentiation of first formed vessels in developing xylem was completed within 1 month after the onset of cambial divisions, whereas the differentiation of first formed fibres took about 2 months (Prislan et al. 2009). This finding is in good agreement with observations of Yoshinaga et al. (1997) on secondary wall thickening and lignification in oak xylem. The same authors also reported that cell wall thickening in oak fibres progressed in two phases, i.e. a faster beginning and a slow second phase. The observations for beech similarly showed that the rate of cell wall thickening was higher during the first weeks and lower during the last weeks. In general and independent of the position within a growth ring, walls of vessels and fibres closer to rays differentiated faster which was also found for conifers (Donaldson 2001).

Electron microscopy was used to follow cell wall formation after cell enlargement by the deposition of polysaccharidic material with subsequent lignification (Fig. 16). Lignin incorporation started in cell corner and radial intercorner middle lamella regions and proceeded centripetally towards the lumen. As the S1 started to lignify during S2 formation, the lignin content still increased in cell corner and intercorner middle lamella regions. The determination of lignin topochemistry by

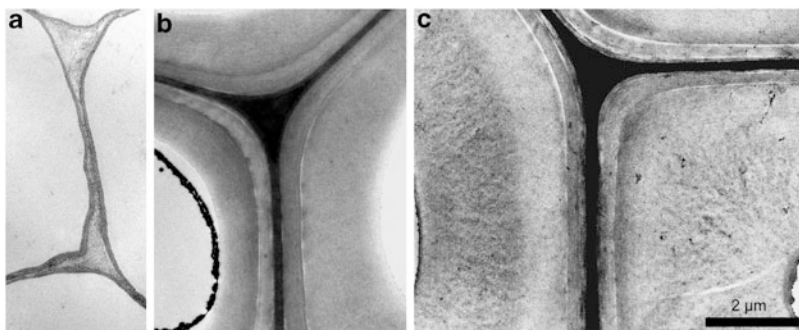


**Fig. 16** TEM micrographs of developing cell walls in beech xylem. (a) Young fibre wall without secondary wall at the end of the enlargement stage with well visible cell corner regions. (b) Secondary wall development of fibres, middle lamella regions and S1 layer completed and S2 layer still developing. (c) Completed wall development showing the typical wall layering of a fibre with broad S2 layer

means of UMSP revealed a homogeneous lignin distribution in the S2 layer of beech fibres as also described by Koch and Kleist (2001). These results were confirmed by TEM analyses of specimens after potassium permanganate staining (Fig. 16).

Point measurements with varying wavelengths were applied for analyses of the lignin composition. The spectra of vessel and fibre walls differed in the position of their maxima with the maxima for vessel walls at a wavelength of around 280 nm, whereas absorbance maxima of fibre walls were at around 278 nm (comp. Fig. 6). This indicates that the walls of these two cell types obviously have a different lignin composition with greater amount of strongly absorbing guaiacyl lignin in vessels and slightly more syringyl units in fibres. Several authors, e.g. Yoshinaga et al. (1997) and Terashima (2000), suggested that the reason for a different chemical composition of fibres and vessels is the successive incrustation of different monolignols (p-hydroxyphenyl, guaiacyl and syringyl) at different stages of differentiation. Yoshinaga et al. (1997) reported that vessel walls of oak showed maximal UV absorbance values at 280–285 nm during cell wall thickening with a shift down to about 273 nm at final stages of their differentiation. Point measurements also revealed that walls of ray and axial parenchyma cells as well as fibres have similarly positioned absorbance maxima at 278 nm.

When comparing the lignin contents of earlywood and latewood fibres of an individual growth ring in beech, latewood fibres displayed slightly higher absorbance values than earlywood fibres. Additionally, a shift of the maximum UV absorbance towards higher wavelengths in latewood fibres points to higher amounts of guaiacyl moieties in these walls as compared to walls of earlywood fibres. Takabe et al. (1992) who analysed the distribution of guaiacyl and syringyl lignin within growth rings of *Fagus crenata* also found that the lignin composition varied within earlywood and latewood. The observations also showed that the differentiation of the last formed fibres continued for approximately 1 month after cessation of

cambial divisions. Similar observations were made for terminal latewood cells of different conifers like *Pinus radiata*, *Abies alba* and *Picea abies* (e.g. Donaldson 1992; Gričar et al. 2005; Gričar and Čufar 2008), but also for *Fagus sylvatica* (Čufar et al. 2008).

### 5.5 Topochemical Studies on Modified Lignin Distribution in the Xylem After Wounding

Wounding of trees induces various responses in woody tissues according to the compartmentalisation concept which is laid down in the so-called CODIT (Compartmentalization Of Damage In Trees) principle (e.g. Shigo and Marx 1977; Liese and Dujesiefken 1996). These responses are divided into passive reactions through structures already existing at the time of wounding (cell walls, cells, rays) and active reactions of living cells (mainly parenchyma cells) stimulated by the wounding (e.g. Schmitt and Liese 1993). Wound reactions are primarily aiming at the protection of inner xylem against air embolism to prevent dysfunction of large portions of the water-conducting system. Well-visible boundary layers consisting of several cell rows with very intensive reactions are finally formed around a wound as barriers against desiccation and the penetration of microorganisms as well as callus tissue which expands from the wound edge to the centre of the wound. Poplar was variously used to analyse wound reactions on a cellular and subcellular level (e.g. Frankenstein and Schmitt 2006). Among various reactions in xylem parenchyma cells, electron microscopy also revealed the formation of modified xylem at the wound edge along a transition zone between xylem formed prior to and after wounding. This zone regularly consists of a high number of unusually thick-walled fibres and could be clearly identified as xylem differentiating at the time of wounding. These modified poplar fibres deposited additional secondary wall (S2) material leading to different patterns of wall thickening. Some of these fibres developed an additional secondary wall layer clearly separated from the S2, whereas others showed a continuously thickened S2 layer (Fig. 17) (details in Frankenstein et al. 2005; Frankenstein and Schmitt 2006). Potassium permanganate staining of ultrathin sections resulted in a relatively strong staining of the secondary wall with heterogeneous lignin distribution within the S2, either with a distinctly darker outer S2 layer or in a patchy appearance of the entire S2 (Fig. 17a, b). These structural features point to an inhomogeneous lignin distribution also within the S2 layer.

The microdistribution of lignin in modified cell walls was also analysed by UV microspectrophotometry (Fig. 18a–c). Scanning analyses at a constant wavelength of 280 nm revealed a relatively low absorbance level for unmodified, thin-walled fibres of poplar and a homogeneous lignin distribution within their various wall layers (Fig. 18a). However, the spectra from modified, thick-walled fibres displayed increased lignin contents and an inhomogeneous lignin distribution. Elevated lignin

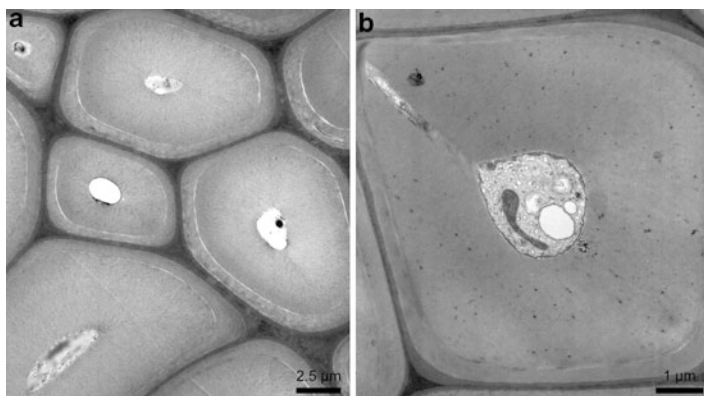


**Fig. 17** Electron micrographs from thick-walled poplar fibres in wound-associated xylem. Secondary wall S2 layers appear enormously thickened (**a** and **b**), whereby potassium permanganate staining resulted in an inhomogeneous staining indicating either a stronger lignification in the outer S2 layer (**a**) or a patchy lignin distribution within the S2 (**b**)

contents were recorded for fibre and vessel walls, whereby the lignin contents increased in the S2 layers of fibres from samples already taken after a few weeks of wound response. This feature appeared more pronounced in samples collected after some months of wound response. The lignin contents in compound middle lamella regions and cell corners mostly were significantly higher.

According to point measurements with varying wavelengths between 240 and 400 nm, absorbance maxima were determined (Fig. 19). At 270–272 nm, fibres from controls showed rather low lignin contents in their S2 layers, as compared with higher absorbance values in the compound middle lamella and cell corner regions. The position of the peak at around 272 is characteristic for a lignin type mainly composed of syringyl units. For modified fibres, the distinctly higher absorbance in their secondary walls and the slightly higher absorbance of the compound middle lamella regions confirmed increased lignin contents. Regarding lignin composition, within thickened secondary walls, the absorbance peak shifted slightly towards higher wavelength because of an increase in guaiacyl moieties and a reduced amount of associated p-hydroxy benzoic acid residues. The same effect was observed for middle lamella regions. The spectra obtained for cell corner regions showed the highest lignin concentrations of predominantly guaiacyl lignin, as deduced from the maximum at around 276–278 nm.

From these results obtained for poplar, it can be stated that in xylem fibres, differentiating at the time of wounding increased wall thicknesses and increased lignin contents and a slightly modified lignin composition may be induced. It is assumed that this wound response is part of the CODIT principle and adds a further mechanism contributing to an increased xylem resistance.



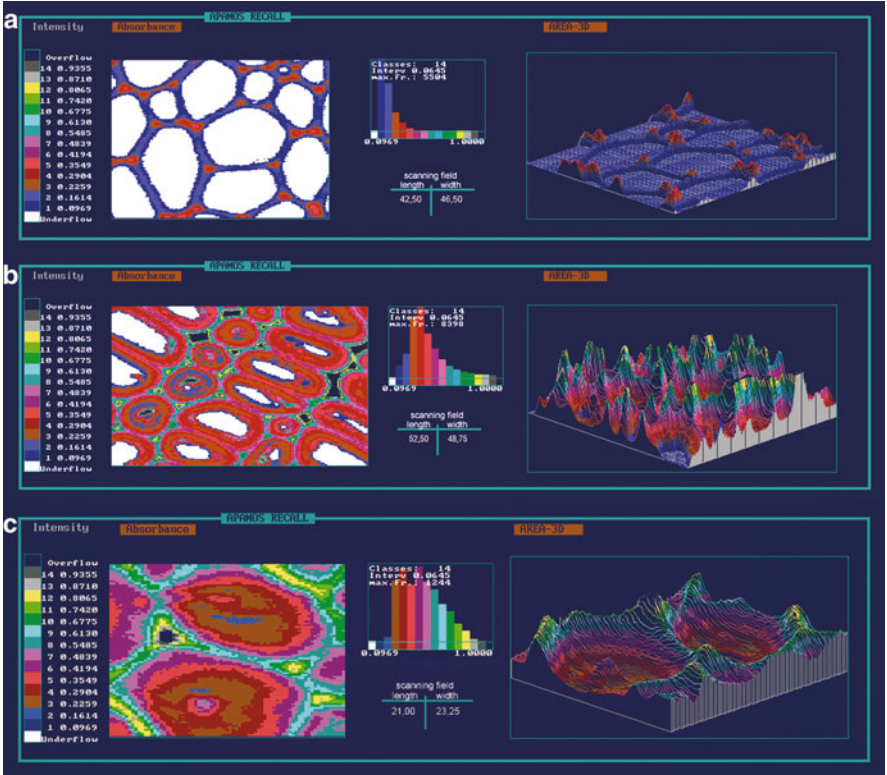


**Fig. 18** UV microscopic image profiles of xylem of unaffected poplar xylem (a) and wound-associated poplar xylem (b and c). In unaffected trees, xylem fibres exhibit thin walls with low absorbance values. Wound-associated poplar xylem at the edge of wounds develops thick-walled fibres with increasing absorbances indicating increased lignin contents in all wall layers (b) and an inhomogeneous lignin distribution (c) (Frankenstein and Schmitt 2006)

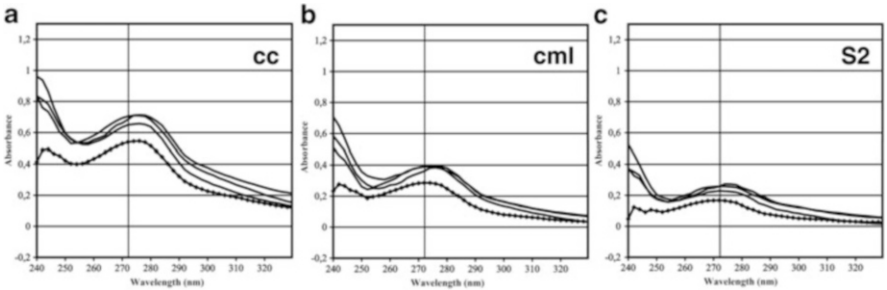


**Fig. 19** Point measurements with representative UV absorbance spectra of individual fibre wall layers (cc cell corner, cml compound middle lamella, S2 secondary wall S2 layer); wound-associated fibres show a generally higher absorbance than control fibres (filled diamond) (Frankenstein and Schmitt 2006)

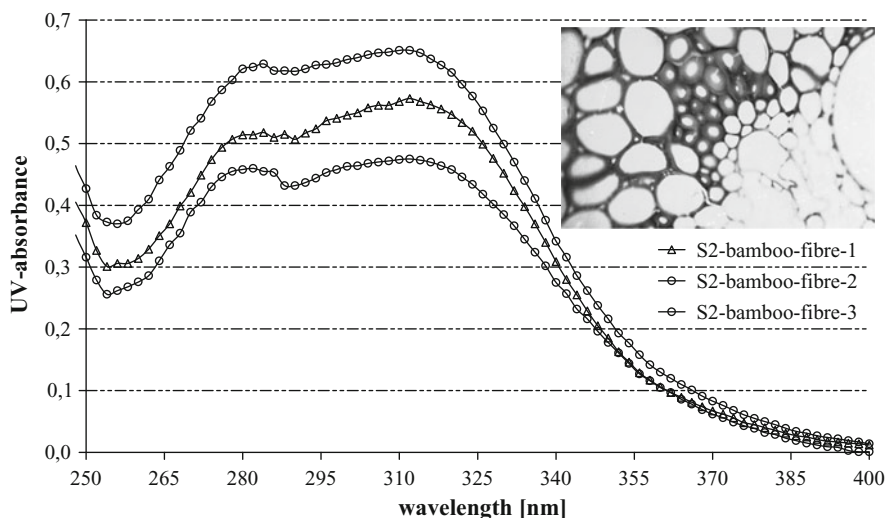


**Fig. 20** UV-absorption spectra of the S<sub>2</sub> cell walls of fibres from a vascular bundle at the middle culm wall

## 5.6 Lignin Distribution in Tropical Bamboo Species

Bamboo lignin is considered to be composed of guaiacyl, syringyl and *p*-hydroxyphenylpropan units. As a unique feature, it also contains 5–10 % of *p*-coumaric acid ester (Higuchi 1987), located at the  $\gamma$ -positions of grass lignin, predominantly in syringyl units (Lu and Ralph 1999).

The distribution of lignin within the cell walls of the tropical bamboo *Gigantochloa levis* was studied topochemically by means of TEM and cellular UV microspectrophotometry (Lybeer and Koch 2005; Lybeer et al. 2006). All spectra curves of the epidermis, fibre, and parenchyma cell walls show a shoulder between 310 and 320 nm (Fig. 20), which can be linked to the presence of *p*-coumaroylation as demonstrated by Higuchi (1987). Most spectra also have an absorbance peak at 280–282 nm, which indicates the presence of the strong absorbing guaiacyl lignin (Fergus and Goring 1970b; Musha and Goring 1975). The UV absorbance of a specific anatomical region depends both on the concentration of the various structural units of lignin and the extinction coefficient of each structural unit. The extinction coefficient of the G (guaiacyl) unit at 280 nm is 3.5 times of that of the S (syringyl) unit (Fergus and Goring 1970a), and the extinction coefficient of the H (*p*-hydroxyphenylpropan) unit is lower than that of the G unit, but higher than that of the S unit (Faix and Schweers 1974). He and Terashima (1991) found a similar guaiacyl peak in the spectra from rice (*Oryza sativa* L.) and sugarcane (*Saccharum officinarum* L.).

In Fig. 21, the lignin distribution within a polylamellated fibre cell wall in mature bamboo is displayed, measured at  $\lambda_{280\text{max}}$ . The lamellation is generally



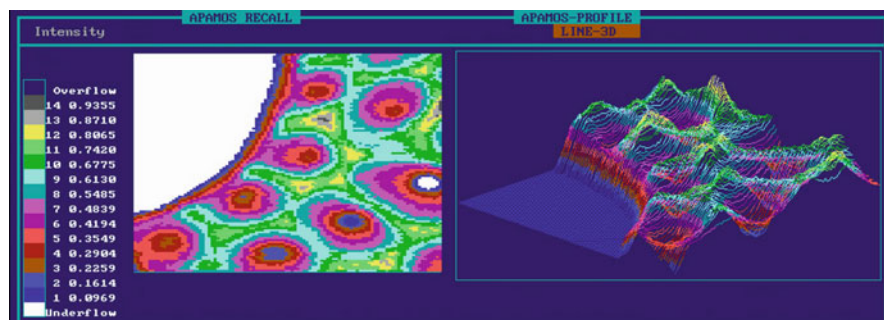


**Fig. 21** UV micrograph and 3D profiles of a bamboo fibre (*P. edulis*) measured at  $\lambda_{280\text{nm}}$

described as alternating broad and narrow layers with different fibrillar orientation. The image profiles show a distinctly high absorbance of the cell corners and compound middle lamellae ( $\text{abs}_{280\text{nm}}$  0.81 to 0.94). The secondary cell wall is characterised by a uniform concentric structure, whereas the absorbance values decrease stepwise from the outer ( $\text{abs}_{280\text{nm}}$  0.74) towards the inner ( $\text{abs}_{280\text{nm}}$  0.29) parts of the wall.

## 6 Conclusions

The described methods and selected examples demonstrate that cellular UV microspectrophotometry and electron microscopy are ideally suited to study the topochemical distribution of lignin and phenolic extractives on a subcellular level. In particular, the application of the UV-scanning technique enables a direct imaging of lignin distribution and provides fundamental information on the topochemistry of lignin. Using these techniques, fine differences in the lignification of individual cell wall layers and the deposition of phenolic extractives can be analysed. The techniques can be used for a wide range of applications in wood biology and topochemistry. Currently, the topochemistry of genetically modified trees as well as thermally and chemically modified wood are studied by using cellular UV spectroscopy and electron microscopy.

## References

- Boerjan W, Ralph J, Baucher M (2003) Lignin biosynthesis. *Annu Rev Plant Biol* 54:519–546
- Brändström J (2001) Micro- and ultrastructural aspects of Norway spruce tracheids: a review. *IAWA J* 22:333–353
- Čufar K, Gričar J, Zupančič M, Koch G, Schmitt U (2008) Anatomy, cell wall structure and topochemistry of water-logged archaeological wood aged 5,200 and 4,500 years. *IAWA J* 29:55–68

- Daniel G, Duchesne I, Tokoh C, Bardage S (2004) The surface and intracellular nanostructure of wood fibres: electron microscope methods and applications. In: Schmitt U, Ander P, Barnett JR, Emons AMC, Jeronimidis G, Saranpää P, Tschegg S (eds) Wood fibre cell walls: methods to study their formation, structure and properties. Swedish University of Agricultural Sciences, Uppsala, pp 87–104
- Dean JFD, Eriksson KE (1994) Laccase and the deposition of lignin in vascular plants. *Holzforschung* 48:21–33
- Donaldson L (1992) Lignin distribution during latewood formation in *Pinus radiata* D. Don. *IAWA Bull* ns 13:381–387
- Donaldson L (2001) Lignification and lignin topochemistry – an ultrastructural view. *Phytochemistry* 57:859–873
- Donaldson L, Ryan KG (1987) A comparison of relative lignin concentration as determined by interference microscopy and bromination/EDXA. *Wood Sci Technol* 21:303–309
- Eriksson I, Lidbrandt O, Westermark U (1988) Lignin distribution in birch (*Betula verrucosa*) as determined by mercuration with SEM- and TEM-EDXA. *Wood Sci Technol* 22:251–257
- Faix O, Schweers W (1974) Vergleichende Untersuchungen an Polymermodellen des Lignins (DPH's) verschiedener Zusammensetzungen. 4. Mitteilung: UV-spektroskopische Untersuchungen. *Holzforschung* 28:94–98
- Fengel D, Wegener G (1989) Wood-chemistry, ultrastructure, reactions. de Gruyter, Berlin
- Fergus BJ, Goring DAI (1970a) The location of guaiacyl and syringyl lignins in birch xylem tissue. *Holzforschung* 24:113–117
- Fergus BJ, Goring DAI (1970b) The distribution of lignin in birch wood as determined by ultraviolet microscopy. *Holzforschung* 24:118–124
- Fergus BJ, Procter AR, Scott JAN, Goring DAI (1969) The distribution of lignin in sprucewood as determined by ultraviolet microscopy. *Wood Sci Technol* 3:117–138
- Frankenstein C, Schmitt U (2006) Microscopic studies on modified wall structure and lignin topochemistry in xylem fibres of poplar after wounding. *Maderas* 8:93–106
- Frankenstein C, Schmitt U, Waitkus C, Eckstein D (2005) Wound callus formation: a microscopic study on poplar (*Populus tremula* L. x *Populus tremuloides* Michx.). *J Appl Bot Food Qual* 79:44–51
- Fromm J, Rockel B, Lautner S, Windeisen E, Wanner G (2003) Lignin distribution in wood cell walls determined by TEM and backscattered SEM techniques. *J Struct Biol* 143:77–84
- Fujii T, Shimizu K, Yamaguchi A (1987) Enzymatic saccharification on ultrathin sections and ultraviolet spectra of Japanese hardwoods and softwoods. *Mokuzai Gakkaishi* 33:400–407
- Fukazawa K (1992) Ultraviolet microscopy. In: Lin SY, Dence CW (eds) Methods in lignin chemistry. Springer, Berlin, pp 110–121
- Glasser WG (1980) Lignin. In: Casey JP (ed) Pulp and paper. Chemistry and chemical technology. Wiley, New York, pp 39–111
- Goldschmid O (1971) Ultraviolet spectra. In: Sarkanen KV, Ludwig CH (eds) Lignins, occurrence, formation, structure and reactions. Wiley, New York, pp 241–266
- Gričar J, Čufar K (2008) Seasonal dynamics of phloem and xylem formation in silver fir and Norway spruce as affected by drought. *Russ J Plant Physiol* 55:538–543
- Gričar J, Čufar K, Oven P, Schmitt U (2005) Differentiation of terminal latewood tracheids in silver fir tracheids during autumn. *Ann Bot* 95:959–965
- Grosser D, Fengel D, Schmidt H (1974) Tamrit-Zypresse (*Cupressus dupreziana* A. CAMUS). Beitrag zur Ökologie, Anatomie und Chemie. *Forstwiss Centralb* 93:191–207
- He L, Terashima N (1991) Formation and structure of lignin in monocotyledons. IV. Deposition process and structural diversity of the lignin in the cell wall of sugarcane and rice plant studied by ultraviolet microscopic spectroscopy. *Holzforschung* 45:191–198
- Hepler PK, Newcomb EH (1963) The fine structure of young tracheary elements arising by redifferentiation of parenchyma in wounded *Coleus* stem. *J Exp Bot* 14:496–503
- Hesse M, Meier H, Zeeh B (1991) Spektroskopische Methoden in der organischen Chemie. Thieme, Stuttgart

- Higuchi T (1987) Chemistry and biochemistry of bamboo. *Bamboo J* 4:132–145
- Higuchi T (1997) Biochemistry and molecular biology of wood. Springer, Berlin
- Hillis WE (1987) Heartwood and tree exudates. Springer, New York
- Hillis WE, Yazaki Y (1973) Polyphenols of *Intsia* Heartwoods. *Phytochemistry* 12:2491–2495
- Jaffé HH, Orchin M (1962) Theory and application of ultraviolet spectroscopy. Wiley, New York
- Joseleau JP, Ruel K (1997) Study of lignification by noninvasive techniques in growing maize internodes. An investigation by Fourier transform Infrared, CP/MAS  $^{13}\text{C}$  NMR spectroscopy and immunocytochemical transmission electron microscopy. *Plant Physiol* 114:1123–1133
- Joseleau JP, Imai T, Kuroda K, Ruel K (2004) Detection in situ and characterization of lignin in the G-layer of tension wood fibres of *Populus deltoides*. *Planta* 219:338–345
- Kim YS, Wi SG, Grünwald C, Schmitt U (2002) Immuno electron microscopic localization of peroxidases in the differentiating xylem of *Populus* spp. *Holzforschung* 56:355–359
- Kindl H (1991) Biochemie der Pflanzen, 3rd edn. Springer, Berlin
- Kleist G, Bauch J (2001) Cellular UV microspectrophotometric investigation of Sapelli heartwood (*Entandrophragma cylindricum* Sprague) from natural provenances in Africa. *Holzforschung* 55:117–122
- Kleist G, Schmitt U (1999) Evidence of accessory components in vessel walls of Sapelli heartwood (*Entandrophragma cylindricum*) obtained by transmission electron microscopy. *Holz Roh Werkstoff* 57:93–95
- Klemm D, Schmauder HP, Heinze T (2002) Cellulose. In: Vandamme E, De Baets S, Steinbüchel A (eds) Polysaccharide II: biopolymers: biology, chemistry, biotechnology, applications, vol 6. Wiley-VCH, Weinheim, pp 277–319
- Koch G, Grünwald C (2004) Application of UV microspectrophotometry for the topochemical detection of lignin and phenolic extractives in wood fibre cell walls. In: Schmitt U, Ander P, Barnett JR, Emons AMC, Jeronimidis G, Saranpää P, Tschegg S (eds) Wood fibre cell walls: methods to study their formation, structure and properties. Swedish University of Agricultural Sciences, Uppsala, pp 119–130
- Koch G, Kleist G (2001) Application of scanning UV microspectrophotometry to localise lignins and phenolic extractives in plant cell walls. *Holzforschung* 55:563–567
- Koch G, Rose B, Patt R, Kordsachia O (2003a) Topochemical investigations on delignification of *Picea abies* [L.] Karst. during alkaline sulfite (ASA) and bisulfite pulping by scanning UV microspectrophotometry. *Holzforschung* 57:611–618
- Koch G, Bauch J, Puls J (2003b) Topochemical characterisation of phenolic extractives in discoloured beechwood (*Fagus sylvatica* L.). *Holzforschung* 57:339–345
- Koch G, Richter HG, Schmitt U (2006) Topochemical investigation on phenolic deposits in the vessels of afzelia (*Afzelia* spp.) and merbau (*Intsia* spp.) heartwood. *Holzforschung* 60:583–588
- Kukkola EM, Koutaniemi S, Gustafsson M, Karhunen P, Ruel K, Lundell TK, Saranpää P, Brunow G, Teeri TH, Fagerstedt KV (2003) Localization of dibenzodioxocin substructures in lignifying Norway spruce xylem by transmission electron microscopy–immunogold labelling. *Planta* 217:229–237
- Kukkola EM, Koutaniemi S, Pöllänen E, Gustafsson M, Karhunen P, Lundell TK, Saranpää P, Kilpeläinen I, Teeri TH, Fagerstedt KV (2004) The dibenzodioxocin lignin substructure is abundant in the inner part of the secondary wall in Norway spruce and silver birch xylem. *Planta* 218:497–500
- Kukkola E, Saranpää P, Fagerstedt K (2008) Juvenile and compression wood cell wall layers differ in lignin structure in Norway spruce and Scots pine. *IAWA J* 29:47–54
- Lange PW (1954) The distribution of the components in the plant cell wall. *Svensk Papperstidn* 57:563–567
- Lehringer C, Gierlinger N, Koch G (2007) Topochemical investigation on tension wood fibres of *Acer* spp., *Fagus sylvatica* L. and *Quercus robur* L. *Holzforschung* 62:255–263
- Lehringer C, Daniel G, Schmitt U (2009) TEM/FE-SEM studies on tension wood fibres of *Acer* spp., *Fagus sylvatica* L. and *Quercus robur* L. *Wood Sci Technol* 43:691–702

- Liese W, Dujesiefken D (1996) Wound reactions of trees. In: Raychaudhuri SP, Maramorosch K (eds) Forest trees and palms-disease and control. Oxford/IBH, New Delhi, pp 20–42
- Lu F, Ralph J (1999) Detection and determination of p-coumaroylated units in lignins. *J Agric Food Chem* 47:1988–1992
- Lybeer B, Koch G (2005) Lignin distribution in the tropical bamboo species *Gigantochloa levis*. *IAWA J* 26:443–456
- Lybeer B, Koch G, Van Acker J, Goetghebeur P (2006) Lignification and cell wall thickening in nodes of *Phyllostachys viridiglaucescens* and *Phyllostachys nigra*. *Ann Botany* 97:529–539
- Maurer A, Fengel D (1991) Elektronenmikroskopische Darstellung von strukturellen Einzelheiten in Nadelholz-Zellwänden anhand sehr dünner Ultramikrotomschnitte. *Holz Roh Werkstoff* 49:53–56
- Michalowicz G, Robert A (1990) The application of transmission electron microscopy for topochemical studies on aspen wood (*Populus tremula*): delignification during soda and soda/AQ pulping. *Holzforschung* 44:39–46
- Musha Y, Goring DAI (1975) Distribution of syringyl and guaiacyl moieties in hardwoods as indicated by ultraviolet microscopy. *Wood Sci Technol* 9:45–58
- Nimz HH (1981) Carbon-13 NMR spectra of lignins, 8 structural differences between lignins of hardwoods, softwoods, grasses and compression wood. *Holzforschung* 35:16–26
- Novaes E, Kirst M, Chiang V, Winter-Sederoff H, Sederoff R (2010) Lignin and biomass: a negative correlation for wood formation and lignin content in trees. *Plant Physiol* 154:555–561
- Parham RA (1974) Distribution of lignin in Kraft pulp as determined by electron microscopy. *Wood Sci Technol* 6:305–315
- Paszner L, Behera NC (1989) Topochemistry of softwood delignification by alkali earth metal salt catalysed organosolv pulping. *Holzforschung* 43:159–168
- Prislan P, Koch G, Schmitt U, Čufar K, Gričar J (2009) Topochemical investigation in developing wood of beech (*Fagus sylvatica*). *Holzforschung* 63:482–490
- Röder T, Koch G, Sixta H (2004) Application of confocal Raman spectroscopy for the topochemical distribution of lignin and cellulose in plant cell walls of beech wood (*Fagus sylvatica* L.) compared to scanning UV microspectrophotometry. *Holzforschung* 58:480–482
- Ruel K (2004) Immunolabelling of lignin sub-structures: a strategy for wood fibre wall topochemical analyses. In: Schmitt U, Ander P, Barnett JR, Emons AMC, Jeronimidis G, Saranpää P, Tschegg S (eds) Wood fibre cell walls: methods to study their formation, structure and properties. Swedish University of Agricultural Sciences, Uppsala, pp 131–140
- Ruel K, Faix O, Joseleau JP (1994) New immunogold probes for studying the distribution of the different lignin types during plant cell wall biogenesis. *J Trace Microprobe Techniques* 12:247–265
- Ruel K, Burlat V, Joseleau JP (1999) Relationship between ultrastructural topochemistry of lignin and wood properties. *IAWA J* 20:203–211
- Saka S, Goring DAI (1988) Localization of lignins in wood cell walls. In: Higuchi T (ed) Biosynthesis and biodegradation of wood components. Academic, New York, pp 51–62
- Saka S, Thomas RJ (1982) Evaluation of the quantitative assay of lignin distribution by SEM-EDXA-technique. *Wood Sci Technol* 16:1–8
- Saka S, Whiting P, Fukazawa K, Goring DAI (1982) Comparative studies on lignin distribution by UV microscopy and bromination combined with EDXA. *Wood Sci Technol* 16:269–277
- Sarkanen KV, Hergert HL (1971) Classification and distribution. In: Sarkanen KV, Ludwig CH (eds) Lignins: occurrence, formation, structure and reactions. Wiley, New York, pp 43–49
- Schmitt U, Liese W (1993) Response of xylem parenchyma by suberization in some hardwoods after mechanical injury. *Trees* 8:23–30
- Schmitt U, Melcher E (2004) Section staining with potassium permanganate for transmission electron microscopy: a useful tool for lignin localisation. In: Schmitt U, Ander P, Barnett JR, Emons AMC, Jeronimidis G, Saranpää P, Tschegg S (eds) Wood fibre cell walls: methods to study their formation, structure and properties. Swedish University of Agricultural Sciences, Uppsala, pp 105–117

- Schmitt U, Singh AP, Frankenstein C, Mölle R (2006) Cell wall modifications in woody stems induced by mechanical stress. *New Zealand J For Sci* 36:72–86
- Scott JAN, Procter AR, Fergus BJ, Goring DAI (1969) The application of ultraviolet microscopy to the distribution of lignin in wood: description and validity of the technique. *Wood Sci Technol* 3:73–92
- Shigo AL, Marx HG (1977) Compartmentalization of decay in trees. USDA For Ser Agric Bull No 405, 74pp
- Singh AP, Donaldson L (1999) Ultrastructure of tracheid cell walls in radiata pine (*Pinus radiata*) mild compression wood. *Can J Bot* 77:32–40
- Smith CG, Rodgers MW, Zimmerlin A, Ferdinando D, Bolwell GP (1994) Tissue and subcellular immunolocalization of enzymes of lignin synthesis in differentiating and wounded hypocotyl of French bean (*Phaseolus vulgaris* L.). *Planta* 192:155–164
- Spurr AR (1969) A low viscosity epoxy resin embedding medium for electron microscopy. *J Ultrastruct Res* 26:31–43
- Takabe K (2002) Cell walls of woody plants: autoradiography and ultraviolet microscopy. In: Chaffey N (ed) *Wood formation in trees*. Taylor and Francis, London, pp 159–177
- Takabe K, Fujita M, Harada H, Saiki H (1981) The deposition of cell wall components in differentiating tracheids of sugi. *Mokuzai Gakkaishi* 27:249–255
- Takabe K, Miyauchi S, Tsunoda R, Fukazawa K (1992) Distribution of guaiacyl and syringyl lignins in Japanese beech (*Fagus crenata*): variation within annual ring. *IAWA Bull* 13:105–112
- Terashima N (2000) Formation and ultrastructure of lignified plant cell walls. In: Kim YS (ed) *New horizons in wood anatomy*. Chonnam National University Press, Korea, pp 169–180
- Terashima N, Fukushima K, Takabe K (1986) Heterogeneity in formation of lignin. VIII. An autoradiographic study on the formation of guaiacyl and syringyl lignin in *Magnolia kobus* DC. *Holzforschung* 40:101–105
- Terashima N, Fukushima K, He L, Takabe K (1993) Comprehensive model of lignified plant cell wall. In: Jung HG, Buxton DR, Hatfield RD, Ralph J (eds) *Forage cell wall structure and digestibility*. Amer Soc Agriculture, Madison, WI, pp 247–270
- Terashima N, Nakashima J, Takabe K (1998) Proposed structure for protolignin in plant cell walls, ACS Symposium Series 697. American Chemical Society, Washington, DC, pp 180–193
- Timell TE (1969) The chemical composition of tension wood. *Svensk Papperstidning* 72:173–181
- Timell TE (1986) *Compression wood in gymnosperms*. Springer, Berlin
- Westermarck U (1985) Bromination of different morphological parts of spruce (*Picea abies*). *Wood Sci Technol* 19:323–328
- Westermarck U, Lidbrandt O, Eriksson I (1988) Lignin distribution in spruce (*Picea abies*) determined by mercurization with SEM-EDXA technique. *Wood Sci Technol* 22:243–250
- Yoshinaga A, Fujita M, Saiki H (1997) Secondary wall thickening and lignification of oak xylem components during latewood formation. *Mokuzai Gakkaishi* 43:377–383



<http://www.springer.com/978-3-642-36490-7>

Cellular Aspects of Wood Formation

Fromm, J. (Ed.)

2013, X, 260 p., Hardcover

ISBN: 978-3-642-36490-7